

# Self-Consistent Modelling of ICRH

T. Hellsten<sup>1,2</sup>, J. Hedin<sup>1</sup>, T. Johnson<sup>1</sup>, M. Laxåback<sup>1</sup> and E. Tennfors<sup>1</sup>

- 1) Division of Fusion Plasma Physics, Alfvén Laboratory, Royal Institute of Technology, SE-100 44 STOCKHOLM, Sweden, Association EURATOM/NFR, <http://www.fusion.kth.se>
- 2) Present address: EFDA-CSU, Culham, OX14 3EA, UK

e-mail contact of main author: [torbjorn.hellsten@jet.efda.org](mailto:torbjorn.hellsten@jet.efda.org)

**Abstract.** The performance of ICRH is often sensitive to the shape of the high energy part of the distribution functions of the resonating species. This requires self-consistent calculations of the distribution functions and the wave-field. In addition to the wave-particle interactions and Coulomb collisions the effects of the finite orbit width and the RF-induced spatial transport are found to be important. The inward drift dominates in general even for a symmetric toroidal wave spectrum in the centre of the plasma. An inward drift does not necessarily produce a more peaked heating profile. On the contrary, for low concentrations of hydrogen minority in deuterium plasmas it can even give rise to broader profiles.

## 1. Introduction

Ion cyclotron resonance heating, ICRH, is a versatile heating method, which can be used not only to heat ions and electrons and provide non-inductive current drive, but also to stabilize or destabilize MHD-modes. The performance is often sensitive to the details of the distribution functions of the heated species, which depend essentially on the strength of the wave field and on the Coulomb collisions [1]. In addition the effects on the distribution function of the finite width of the drift orbits and of the RF-induced spatial transport are important. Depending on the direction of wave propagation this transport can either curtail or enhance the high-energy part of the distribution function [2]. Since the wave field and distribution functions depend on each other, they have to be calculated self-consistently. Here, we present results from such computations with the SELFO code [3] for the standard heating scenario of hydrogen minority in deuterium plasma.

## 2. The evolution of the drift orbits due to wave particle interactions

In order to study the evolution of the distribution function for weakly colliding ions during ICRH, it is convenient to express the distribution function as a set of drift orbits, defined by their invariants of motion. In the present work the following invariants are used:  $E = mv^2/2$ ,  $\Lambda = \mu B_0/E$  and  $P_\phi = mRv_\phi + q\Psi$ . Particles traveling parallel,  $v_\parallel > 0$ , and anti-parallel,  $v_\parallel < 0$ , to the magnetic field are denoted co- and counter-passing, respectively. The plasma current is chosen to be antiparallel with the magnetic field.

The changes in the energy  $E$  due to wave-particle interactions are determined by the wave field and the phase difference between the wave and the gyro angle. The changes in  $\Lambda$  and  $P_\phi$  are determined by the change in energy,  $\Delta E$ , [4];  $\Delta\Lambda = (n\omega_{c0}/\omega - \Lambda)\Delta E/E$  and  $\Delta P_\phi = n_\phi\Delta E/\omega$ , where  $n$  is the harmonics of the cyclotron frequency,  $n_\phi$  the toroidal mode number,  $\omega$  the angular frequency of the wave and  $\omega_{c0}$  the angular cyclotron frequency at the magnetic

axis. By integration we obtain the characteristics, along which the motion in the invariant space  $(E, \Lambda, P_\phi)$  is constrained

$$(E, \Lambda, P_\phi) = \left( E, \frac{n\omega_{c0}}{\omega} + \frac{C_2}{E}, \frac{n_\phi}{\omega}E + C_1 \right) \quad (1)$$

Coulomb collisions will change  $E$  and the two integration constants  $C_1$  and  $C_2$ . For a single  $n_\phi$  the RF-interactions describe diffusion along a curve in the invariant space. As the energy increases  $\Lambda$  will be driven towards  $\Lambda_{\text{res}} = n\omega_{c0}/\omega$ , i.e. the turning point of the trapped ions are driven towards the cyclotron resonance. The flux surface of the turning points of a trapped orbit is determined by

$$\Psi_T = \frac{m}{q} \left( \frac{n_\phi}{\omega}E + C_1 \right) \quad (2)$$

The change in the radial location of the wave-particle interaction at the Doppler shifted cyclotron resonance is given by [5]

$$\frac{\Delta R}{R} = \left( \frac{\omega - n\omega_c}{\omega} \right)^2 \frac{1}{1 + \Lambda \frac{R_c}{R} \left( \frac{n\omega_c}{\omega} - \frac{3}{2} \right)} \frac{\Delta E}{2E} \quad (3)$$

The interactions will shift towards the low field side as the energy increases. Thus, the locations of the interactions on the high field side will move towards the unshifted cyclotron resonance whereas on the low field side they will move away from the resonance. From Eq. (1) it follows that waves having  $n_\phi > 0$  drive resonating ions on trapped orbits outwards and waves having  $n_\phi < 0$  inwards, resulting in an inward and an outward particle drift, respectively. In a first approximation a symmetric spectrum provides no toroidal momentum input and the drifts should cancel, leaving only a RF-induced diffusive transport. However, due to the Doppler shift the wave-particle interactions will take place at different spatial locations with different field strength and therefore the inward and outward drift terms will, in general, not cancel. In some regions of the invariant space the ions interact only with the positive or negative  $n_\phi$ .

### 3. Self-consistent calculations of the velocity distribution and the wave field

The SELFO code [3] calculates self-consistently the distribution function and the wave field. The wave field is calculated with the LION code [6, 7], which is a global wave code computing fast and shear Alfvén waves in the ion cyclotron frequency range for a prescribed dielectric tensor. The FIDO code [8] is a parallelized Monte Carlo code calculating the orbit averaged distribution function of the resonating ions in a toroidal geometry, expressed in the invariants  $(E, \Lambda, P_\phi)$  using the computed wave field and the partition of the absorbed power as input. Finite orbit widths and RF induced spatial transport are included in FIDO. Fully decorrelated wave-particle interactions, as described in FIDO, is consistent with the response described by a dielectric tensor and a quasi-homogeneous wave field. The contribution to the dielectric tensor from the resonating ions is calculated from the distribution function obtained with FIDO and then included in the dielectric tensor used in LION to calculate the wave field. Self-consistent calculations are obtained by repeating this procedure in an iterative manner.

### 4. Minority hydrogen heating in deuterium plasmas

We analyze the standard scenario of minority hydrogen heating in a deuterium plasma having the cyclotron resonance on the high field side with the following parameters:  $B_0 = 2.08$  T,  $R_0 =$

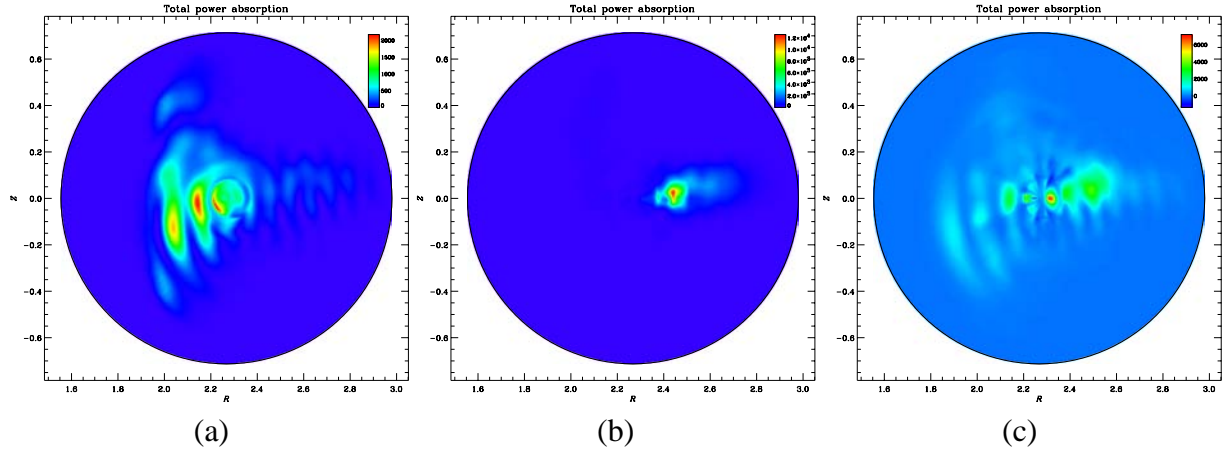


FIG. 1: The power absorption for  $n_\phi = -30$  at  $t = 0$  s (a) and  $t = 0.2$  s (b) and for  $n_\phi = 30$  at  $t = 0.2$  s (c).

2.28 m,  $a = 0.75$  m,  $I_p = 0.75$  MA,  $f = 34$  MHz,  $n_\phi = -30$ ,  $P = 5$  MW,  $n_{D0} = 4 \cdot 10^{19}$  m $^{-3}$ ,  $n_H/n_D = 5$  %,  $T_i = T_e = 5$  keV. Because of the strong damping the total hydrogen absorption does not change significantly, but the wave field and the distribution function of the hydrogen ions do. Initially the distribution is thermal and the absorption is localized around the cyclotron resonance. After 0.2 s, when the tail has developed, the distribution function of ions with energy above 50 keV is composed of 12 % trapped orbits, 60 % potato orbits and 18 % non-standard passing orbits residing on the low field side. The latter ions have the highest energy. The change in the power deposition can be seen in Fig. 1a and b [5].

Waves with  $n_\phi = 30$  will as in the former case drive the ions into trapped banana orbits, but since the RF-induced transport drives the ions outwards fewer non-standard orbits are obtained and the high energy tail is dominated by standard trapped ions. The shift of the power absorption towards the low field side is for this case smaller, as can be seen in Fig. 1c. This is due to the wave-particle interactions taking place on the inner leg.

For a symmetric spectrum the inward and outward drift terms do not cancel. Instead of a weak outward spatial diffusion, which is expected if the drift terms would have cancelled, the inward drift will dominate, producing a large fraction of non-standard orbits [9].

## 5. Current drive

Both electron and ion currents can be driven by the magnetosonic wave. For fast wave current drive by electrons it has been shown that the formation of a high-energy tail of parasitically heated ions due to the presence of higher harmonic resonances strongly reduces the power absorbed by electrons and thereby the driven electron current [3]. In this case the ion cyclotron absorption is strongly enhanced by the presence of the inward drift producing asymmetries of the fast wave current drive with respect to the toroidal phasing, which are consistent with experimental observations.

For minority current drive the finite orbit width and RF-induced spatial transport introduces new mechanisms for driving ion current [10, 11]. Thereby the symmetry of the current drive profiles and efficiencies with respect to mode spectra and heating at the LFS and HFS of the magnetic axis [12] disappears, as shown in Fig. 2 for minority hydrogen heating in a JET-like deuterium plasma with  $B_0 = 2.52$  T,  $R_0 = 3.0$  m,  $a = 1.25$  m,  $I_p = 2.0$  MA,  $f = 42.7$  MHz,  $P = 5$  MW,  $n_{D0} = 2.7 \cdot 10^{19}$  m $^{-3}$ ,  $n_H/n_D = 8$  %,  $T_i = T_e = 5.5$  keV. For cases with  $n_\phi = 15$

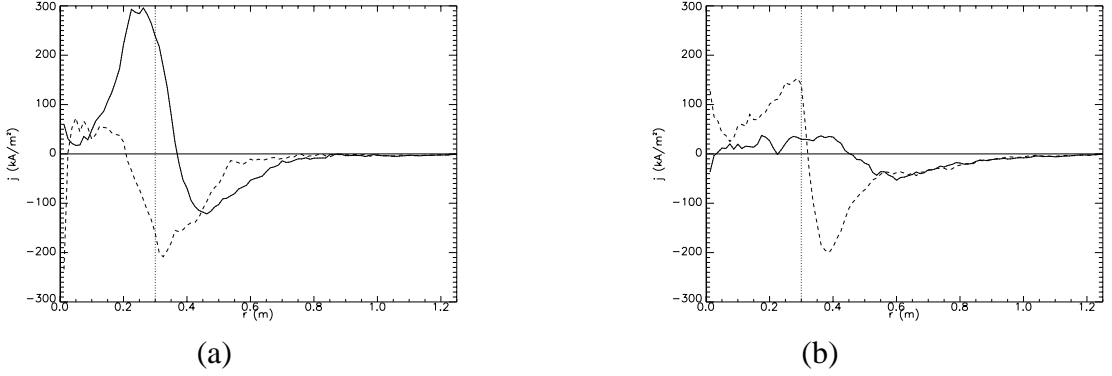


FIG. 2: Ion cyclotron current drive on the high field side (a) and low field side (b). Solid line for  $n_\phi = 15$  and dashed line for  $n_\phi = -15$ . The dotted line marks the cyclotron resonance.

on the HFS and  $n_\phi = -15$  on the LFS the driven currents have bipolar profiles similar to those by [12, 13], but with different magnitudes. For the other two cases there are no similarities. These results are consistent with sawtooth stabilisation at JET [13]. At the high field side, current drive by passing particles dominates, whereas at the low field side it is dominated by trapped ions. The new current drive mechanisms enable on axis current drive as well as current drive with a symmetric spectrum [11].

The spread of the wave field along and across the resonance requires self-consistent computations of the distribution function and the wave field. In general the detrapping of resonating ions, being an important mechanism for the current drive [11, 14], is slightly reduced for self-consistent computations because of the weaker wave field strength on the high field side of the resonance.

## 6. Heating of plasmas with ITBs

A semi-empirical transport model [15, 16] has recently been coupled to SELFO, enabling predictive modelling of heating with internal transport barriers, ITBs. Because of the low poloidal magnetic field in the centre and the high energy of the ions the effect of the orbit width becomes particularly important for the power deposition for these discharges.

An inward RF-induced drift should lead to better confinement of the high energy ions as well as a more peaked power deposition [2, 17]. However, the RF-induced drift also affects the partition of power absorbed on hydrogen and deuterium. For small hydrogen concentrations the outward drift will reduce the power absorbed by hydrogen and increase the power absorbed by the deuterium ions at their second harmonic resonance. The power absorbed by the thermal deuterium ions and by the high energy part of the bulk will then give rise to a peaked central power deposition and more ion heating, as can be seen in Fig. 3, showing a JET-like plasma at  $t = 1s$  with an ITB at  $r/a = 0.55$ .  $B_0 = 2.6T$ ,  $f = 39.5\text{ MHz}$ ,  $n_{D0} = 2.6 \cdot 10^{19}\text{ m}^{-3}$ ,  $n_H/n_D = 1\%$ ,  $P_{ICRH} = 7.5\text{ MW}$  and  $P_{NBI} = 7.5\text{ MW}$ .

## 7. Conclusions

The performance of many ICRH scenarios strongly depends on the details of the distribution functions of the resonating species. To correctly describe these often requires self-consistent calculations of the wave field and the distribution functions. The effects of the finite orbit width and the RF-induced spatial transport can often be crucial for the performance.

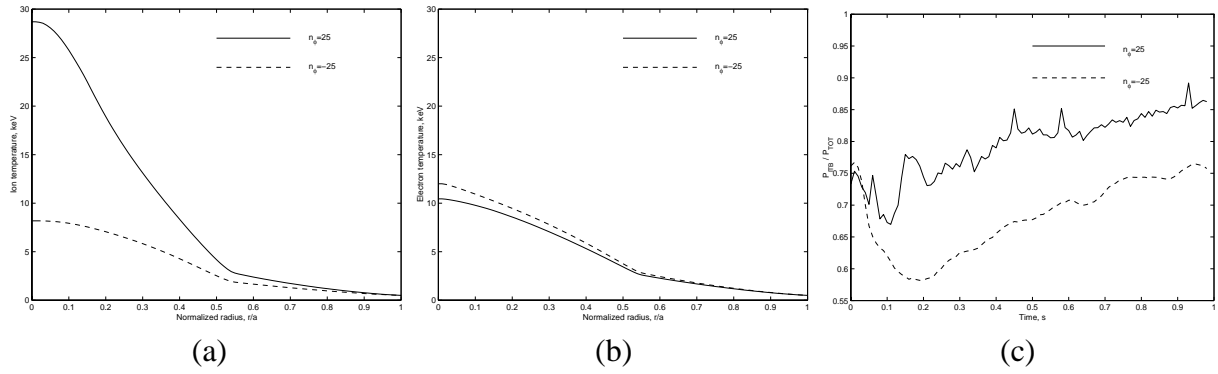


FIG. 3: Ion (a) and electron (b) temperatures for  $n_\phi = 25$  (solid line) and  $n_\phi = -25$  (dashed line). The fraction of the ICRH power deposited within the ITB can be seen in (c).

Due to the Doppler shift the wave-particle interactions take place in different parts of the phase space with waves propagating either co or counter to the magnetic field. As a result, plasmas heated with a symmetric toroidal wave spectrum experience a dominating inward drift in the centre of the plasma.

For ion cyclotron current drive the finite orbit width and the RF-induced spatial transport produce driven current profiles that in many cases are very different from those given by [13].

The inward drift of the resonating ions does not necessarily produce a more peaked heating profile. For low concentrations of hydrogen minority in deuterium plasmas, it can give rise to a broader profile because the hydrogen tail has wider orbits than the deuterium tail.

## 8. References

- [1] T.H. Stix, *Nuclear Fusion*, **15** 737–754 (1975)
- [2] M.A. Kovanen et al., *Nuclear Fusion*, **32** 787 (1992)
- [3] J. Hedin, et al., In *Theory of Fusion Plasmas 1998*, pages 467–472, Varenna, (1999), ISBN 88-7794-167-7
- [4] L.G. Eriksson et al., *Physics of Plasmas*, **6** 513 (1999)
- [5] J. Hedin, et al., *Nuclear Fusion*, **40** 1819 (2000)
- [6] L. Villard, et al., *Computer Physics Reports*, **4** 95 (1986)
- [7] L. Villard, et al., *Nuclear Fusion*, **35** 1173 (1995)
- [8] J. Carlsson, et al., In *Proceedings of the Joint Varenna-Lausanne Workshop “Theory of Fusion Plasmas”*, page 351, (1994)
- [9] J. Hedin, et al., In *Theory of Fusion Plasmas 2000*. Joint Varenna-Lausanne International Workshop, (2000)
- [10] T. Hellsten, et al., *Physical Review Letters*, **74** 3612–3615 (1995)
- [11] J. Carlsson, et al., *Physics of Plasmas*, **5** 2885–2892 (1998)
- [12] N. J. Fisch, *Nuclear Fusion*, **21** 15–22 (1981)
- [13] V. P. Bhatnagar et al., *Nuclear Fusion*, **34** 1579 (1994)
- [14] T. Johnson, et al., In *to appear in the Proceedings of ICCP in Quebec*, (2000), BP1.157
- [15] M. Laxåback, Technical report, Alfvén Laboratory — Royal Institute of Technology, (2000), ISSN 1102-2051
- [16] V.V. Parail et al., Technical Report JET-P(98)50, JET Joint Undertaking, Abingdon, Oxfordshire, OX14 3EA, UK, (1998)
- [17] L.-G. Eriksson, et al., *Physical Review Letters*, **81** 1231–1234 (1998)